

# Cytometry investigation of myo-inositol-induced growth inhibition, apoptosis induction and cell cycle arrest in the human prostate cancer cell line (DU-145).

M. J. Islam<sup>1</sup>, Adhir Kumar Das<sup>2</sup>, Muntaha.S<sup>3</sup>

## ABSTRACT

### Background

Prostate cancer remains the second most frequent diagnosed cancer in men and is the third leading cause of cancer related death, despite many available treatment options. The use of dietary supplements to prevent this cancer is one method of controlling it. Myo-inositol, a dietary component, has been shown to have cancer-chemopreventive properties against a variety of experimental cancers, however few research have been conducted, and molecular mechanisms are unclear.

### Methods

In the current study, we investigated at the growth-inhibitory properties of myo-inositol and associated mechanisms in the androgen-independent human prostate cancer DU-145 cells. After 48 hours of treatment with myo-inositol, cytological studies using an inverted phase contrast microscope and Hoechst 33342/PI dual-staining assay revealed characteristic apoptotic morphology of cancer cells. MTT assay against mouse lung fibroblast (L-929) cell line and trypan blue dye exclusion assay against human prostate cancer (DU-145) cells were used to determine cytotoxic efficacy. Flow cytometry and FITC/PI labelling were used to confirm the presence of apoptosis.

### Results

The growth inhibitory effect and the  $IC_{50}$  value were demonstrated by myo-inositol at 0.06 mg/ml (\*\* $p < 0.05$ ). It is suspected that cell deaths are related to apoptosis induction and cell-cycle arrest. Treatment with Myo-inositol has been further identified by induction of early and late apoptosis (\*\* $p < 0.01$ ). Apoptosis can also be detected using DNA fragmentation and Hoechst 33342 fluorescent dye stain analysis. Myo-inositol caused an alteration to the cell cycle regulation on DU-145 cell line at G0/G1 and S phase, respectively (\*\* $p < 0.01$ ).

### Conclusion

These molecular and cytometric alterations shed light on how myo-inositol produces statically significant growth inhibition, G1-S phase arrest, and late apoptotic cell death in human prostate cancer DU145 cells.

### Keywords:

Myo-inositol; Apoptosis; cell cycle arrest; Cancer-chemoprevention.

## INTRODUCTION

The global burden of cancer is increasing at an alarming rate, putting enormous strain on the general public and health systems at all levels of the economy. Cancer is the greatest cause of illness and death worldwide, independent of geographic diversity or human developmental status, primarily because of the extended period curative and palliative treatment measures, which can be rather expensive, together with the important misfortune due to morbidity and mortality<sup>1,2</sup>. According to the WHO Global Cancer Observatory (GLOBOCAN, 2020) there are around 10.0 million cancer deaths and 19.3 million new cancer cases reported in 2020. Prostate cancer is the second most common cancer among males and the fifth major cause of cancer mortality in 2020. Worldwide, an estimated 1.4 million new cases and 55,000 deaths have been reported<sup>3-5</sup>. Furthermore, the incidence rate varies across the region, ranging

1. M. J. Islam , Associate Professor of Pharmacology, Bangabandhu Sheikh Mujib University (BSMMU), Dhaka, Bangladesh.
2. Adhir Kumar Das, Professor of Pharmacology, Bangabandhu Sheikh Mujib University (BSMMU), Dhaka, Bangladesh.
3. Muntaha.S, Lecturer, Shahabuddin Medical College, Gulshan, Dhaka.

## Correspondence

Dr Mohammad Jahidul Islam, Associate Professor of Pharmacology. Bangabandhu Sheikh Mujib University (BSMMU), Dhaka, Bangladesh.  
E-mail: [jahidul\\_islam@bsmmu.edu.bd](mailto:jahidul_islam@bsmmu.edu.bd)

from 6.3 to 83.4 per 100,000 males, with the highest rates in Northern and Western Europe and the lowest in Asia and North Africa. Prostate cancer frequency is significant among men aged >65 years, suggesting that the advancing age is a considerable detrimental condition for prostate cancer occurrence, categorized as a non-modifiable risk factor. Moreover, positive family history is essential, but known genes presently explain only 35% of the familial risk, those patients present with regards to a positive family history of PCa; they are at intensified 60% possibilities of developing PCa. Race, diet, inflammation, and hormonal components are all other risk factors for prostate cancer<sup>6,7</sup>. As for the illustration, African American men are 1.6 occasions bound to be determined to have prostate malignancy and are twice as liable to terminate from the sickness as white men in the USA.

Dietary factors, a significant factor that can modify cancer risk in a few assorted manners at multiple stages of the carcinogenic course<sup>8</sup>. Several foods, nutrients and lifestyle have been associated to the inhibition of development of prostate cancer by the compounds with antioxidant action, arresting cell cycle or by inducing apoptosis, an essential role in the prevention of PCa. Myo-inositol, commonly known as phytic acid, is an essential component of a natural diet and is described as a “natural carcinogen fighting warrior”<sup>9,10</sup>. That is all Abundant in fiber-rich diets. In many cancer models, nearly three decades of study on myo-inositol have revealed this broad-spectrum antineoplastic effect. In cell culture, myo-inositol inhibits 1) human breast, colon, and liver cancer cells, as well as rhabdomyosarcoma and erythroleukemia cells, and 2) mouse epidermal JB6 cell transformation. Myo-inositol has also been demonstrated to inhibit phorbol ester- or epidermal growth factor-induced ERK1/2-AP1. JB6 cells utilise the activation and activity of phosphatidylinositol-3 kinase (PI-3K) as a tumor-promoting mechanism<sup>10,11</sup>. Regarding the *in vivo* anticancer efficacy of myo-inositol, it has been found that 1% IP6 in drinking water administered a week before or two weeks after Azoxymethane administration inhibits the growth of colon cancer in F344 rats<sup>12,13</sup>. Later, it was discovered that treatment of the same animal model with 2% IP6 in drinking water dramatically reduces the frequency and size of large intestine tumours, even after 5 months of carcinogen induction. Myo-inositol has also been reported to prevent CD-1 mice from developing dimethylhydrazine-induced colon cancer<sup>14,15</sup>. Since,

at an advanced stage, PCA growth and development become androgen independent, rendering androgen ablation therapy ineffective, it is extremely important to manage PCA by chemoprevention and intervention techniques<sup>16,17</sup>. Currently, we are evaluating the effectiveness of myo-inositol on cell growth, cytotoxicity, cell cycle progression, apoptotic cell death, and associated morphology and processes. The result obtained demonstrate that myo-inositol inhibits DU-145 cell growth and proliferation, along with G1-S phase arrest (\*\*\*) $p < 0.01$  through flowcytometric analysis. Induction of early and late apoptosis has been discovered as an additional effect of Myo-inositol treatment (\*\*\*) $p < 0.01$ . DNA fragmentation and Hoechst 33342 fluorescent dye stain analysis can also identify apoptosis.

## MATERIALS AND METHODS

### Cell line and reagents

American Type Culture Collection (Manassas, VA) provided the human prostate cancer DU-145 and Mouse Skin Fibroblast Cell Line (L929) cell line. The DU-145 cell lines were cultured in the Minimum Essential Medium (MEM). The procurement of myo-inositol from Sigma-Aldrich Chemical Co. (Germany). Fetal Bovine Serum (FBS), MEM, trypsin, Phosphate-Buffered Saline (PBS), Penicillin-Streptomycin were purchased from Life Technologies, USA. Cell culture T25 flasks, pipettes, trypsin EDTA (1x), were purchased from Sigma- Aldrich (Germany). The other chemical materials such as 2% lysis buffer (Tris-HCl 100 mM, EDTA 20 mM, NaCl 1.4 M), Annexin V-FITC apoptosis detection kit, Hoechst 33342 fluorescent dye was obtained from Life Technologies, USA. 100 mM of Myo-inositol hexakisphosphate dodecasodium salt (Sigma-Aldrich, St. Louis, Missouri, United States) was added. With water, the stock solution is diluted.

### Cell culture and myo-inositol treatment

DU-145 cells were placed on 6-wall plates in  $1 \times 10^5$  cell counts and were cultured in MEM medium under conventional culture conditions (37° degrees Celsius, 95% relative humidity, and 5% carbon dioxide) for 72 hours. MEM medium was supplemented with 10% Fetal Bovine Serum (FBS) and 1% Penicillin-Streptomycin. Then, cells were treated with varied concentrations (0.2–1.0 mg/ml) of myo-inositol (pH 7.4) dissolved in distilled water at various times (24–72 h). Cell proliferation analysis were performed to scrutinize the

anti-proliferative effect of Myo-Inositol. Control cells were cultured in growth media without any treatment. Viable cell numbers measured using the Trypan Blue Exclusion and MTT Assay (TBEA) suggest that the  $IC_{50}$  dose of Myo-inositol (0.06 mg/ml) relative to untreated cells for 8 days significantly suppressed DU-145 cell proliferation. This study showed that similar results could be found in three different experiments.

### Cell cytotoxicity assay

In each well for 24 hours, a total of  $3 \times 10^4$  the fibroblast cell line of mouse skin (L929) cells was seeded into six well plates, this cell line was chosen because it provides many long-term compatible cells with most constant cellular features. The cells were then treated with an  $IC_{50}$  dose of Myo-inositol compound and were administered for 72 hours. Cells were washed once with PBS after 72 hours of incubation period, trypsinized, and neutralised with a fully freshly prepared medium. At  $200 \times g$  for 5 min, the cell suspensions were concentrated. The supernatant was removed and replaced with 1 ml of the entire new medium. Cell numbers were calculated by using the TBEA method<sup>18,19</sup>.

### DNA fragmentation analysis

On six well plates for 24 hours, DU 145 cells numbered  $1.0 \times 10^5$  were seeded. The cells were treated for 72 hours following incubation with an  $IC_{50}$  dose of Myo-inositol compound. The cells were harvested and washed with PBS after therapy. The DMSO (100  $\mu$ l) was then directly applied to the cell pellet and thoroughly mixed by vortexing. A TE buffer (pH 7.4) of equal volume (100  $\mu$ l) with 2% SDS was applied and mixed by vortexing. The resulting solution was centrifuged at  $12,000 \times g$  at  $4^\circ C$  84 and 40  $\mu$ l of the supernatant was loaded with 2% agarose gel. UV-spectroscopy was used to analysed the isolated DNA<sup>20</sup>.

### Hoechst 33342 stain analysis

On six well plates for 24 hours, DU 145 cells numbered  $1.0 \times 10^5$  were seeded. The cells were treated for 72 hour following incubation with an  $IC_{50}$  dose of Myo-inositol compound. The cells were extracted and washed after treatment three times with PBS. The cells were incubated for 30 minutes at room temperature with the Hoechst 33342 stain. The cells were rinsed with PBS three times after aspirating the stain before being viewed under UV fluorescence microscopy at a wavelength of 498 nm<sup>21</sup>.

### Flow cytometry analysis for apoptosis induction and cell cycle arrest

Trypsinize cells with 1 ml of trypsin-EDTA at  $37^\circ C$  for 5-10 minutes, or until cells are totally detached. The medium was then replaced with 3 ml of 10% FBS-MEM to terminate the trypsinization of medium. It was then pipetted carefully to prevent cellular clumps. The cells are spun down in a centrifuge for 5 minutes at 1000 rpm after being transferred to an Eppendorf tube. Cells were rinsed with phosphate-buffered saline (1X) and the supernatant was discarded. The cells were subsequently treated with the  $IC_{50}$  concentration of myo-inositol (0.06 mg/ml) and then collected and resuspended in 100  $\mu$ L of Annexin V binding buffer. 5  $\mu$ L of Annexin V-FITC was subsequently added. Following a 15-minute incubation at room temperature in the dark, cells were centrifuged at 1,000 rpm for 5 minutes. The cell pellet was then resuspended in 200  $\mu$ L Annexin V binding buffer and counterstained with 5  $\mu$ L propidium iodide (PI) before to analysis. Using FACS-Calibur flow cytometry, the cells were investigated (Becton Dickinson, San Jose, USA). 515–545 nm emission filter for FITC (green) and 600 nm for PI (red). Total events per 10000 sampled cells were collected and analysed using Cell Quest Software (UKM, Malaysia). Following each treatment, cells were collected after a brief incubation with trypsin-

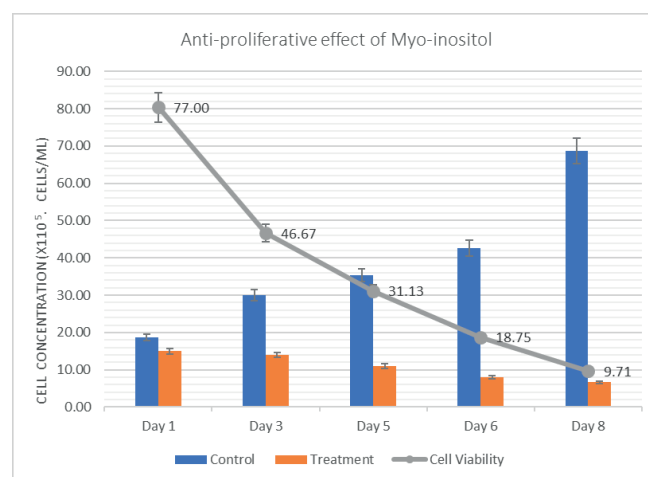


**Figure 1:** Antiproliferative effect of Myo-inositol correspond to the time. The cells were treated at  $IC_{50}$  of Myo-inositol until 8 days with growth medium renewal on day 3 and day 6. Percentages of cell viability and number of cell concentration upon treatment with Myo-Inositol compound. Data shown are mean  $\pm$  standard deviation (SD) of triplicate experiments.



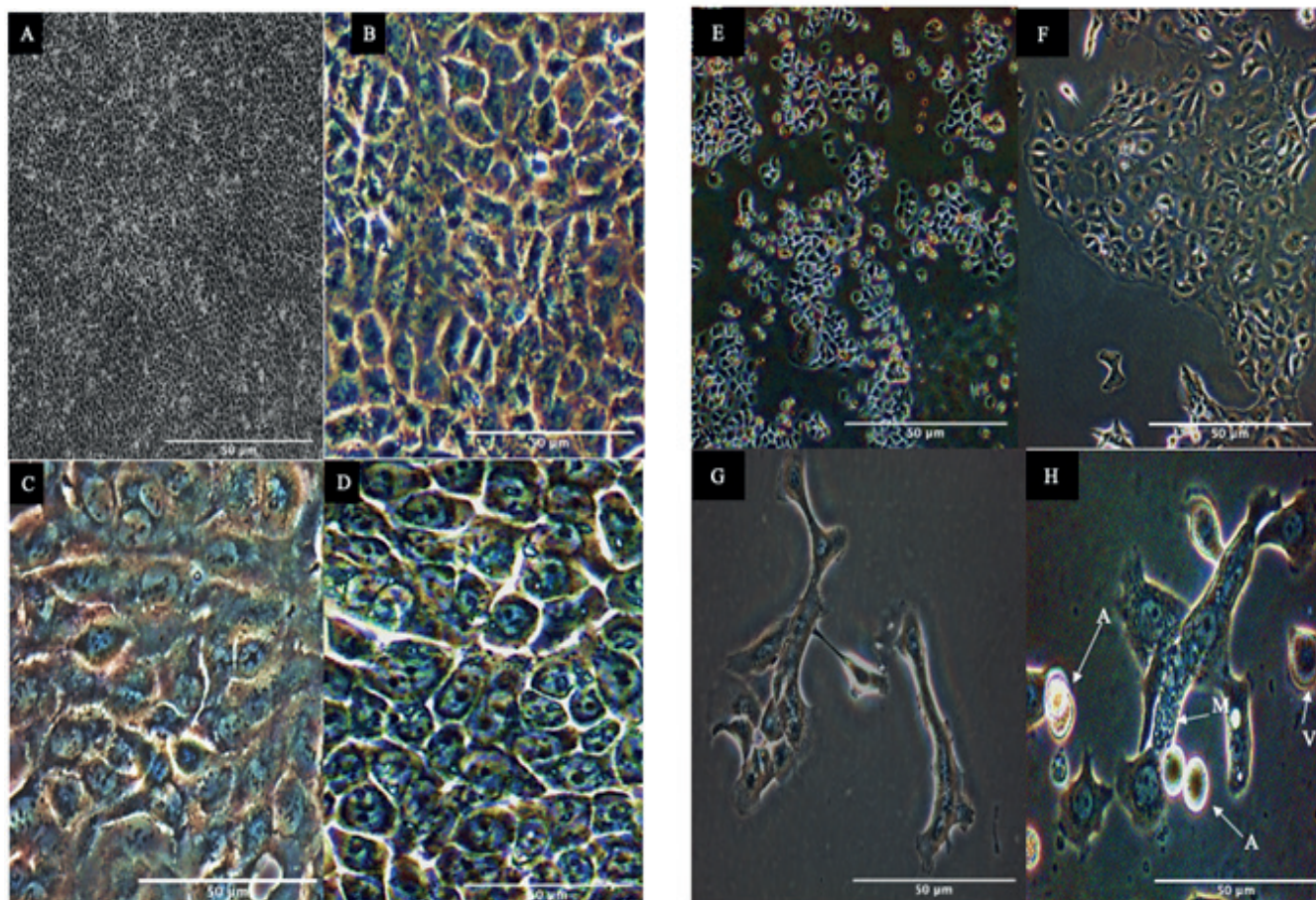


**Figure 2:** Cell morphology of DU-145 cells without treatment (Control group) of Myo inositol with various magnification (A) 40X, (B), 100X (C) 200X and (D) 400 X. Cell morphology of DU-145 cells with  $IC_{50}$  dose of Myo-inositol treatment. There are few apoptotic morphological changes seen showing various magnification (E) 40X, (F) 100X (G) 200X and (H) 400 X. Cell shrinkage (C), membrane blebbing (M), vacuolization(V), cell elongation (L), and apoptotic bodies (A).

EDTA. Cell cycle analysis was then performed.  $1 \times 10^5$  cells were suspended in 0.5 ml saponin/propidium iodide (PI) solution (0.3% saponin (wt/vol), 25 mg/ml PI (wt/vol), 0.1 mM EDTA, and 10 mg/ml RNase (wt/vol) PBS) and incubated overnight at 4<sup>o</sup> Celsius in the dark room. Flow cytometry was then utilised to study cell cycle distribution at the University of Science Malaysia utilising FACS analysis (USM, Malaysia). ModFit LT Cell Cycle Analysis Software was then used to determine the percentage of cells in each phase of the cell cycle<sup>22,23</sup>.

## RESULTS

### Cell proliferation analysis of Myo-Inositol on DU-145 Cells

DU-145 Prostate cancer cells were grown on 6-well plates  $1.0 \times 10^5$  cells, and the dose-dependent response

was tested using trypan blue excision assay (TBEA) during 72 hours of treatment and MTT assay. Stock solution 50 mg/ml of the Myo-inositol compound were diluted with MEM media supplemented with 10% heat-inactivated FBS at concentration of 0.02 mg/ml, 0.04 mg/ml, 0.06 mg/ml, 0.08 mg/ml, and 0.10 mg/ml respectively. Different concentrations of Myo-inositol solution were tested on DU-145 cells for 72 hours (3 days) of incubation (Table 1). The  $IC_{50}$  dose was 0.06 mg/ml. The Myo-inositol solution affected DU-145 cells in a dose-based manner and the  $IC_{50}$  dose decreased cell viability by 50.26%. In DU-145 cells, the Myo-inositol aqueous solution has an effective inhibitory effect ( $**p < 0.05$ ) and potency.

As shown in the Figure 1, the anti-proliferative effect of Myo-inositol was in dose and time dependent manner. The cell proliferation has continuously been inhibited

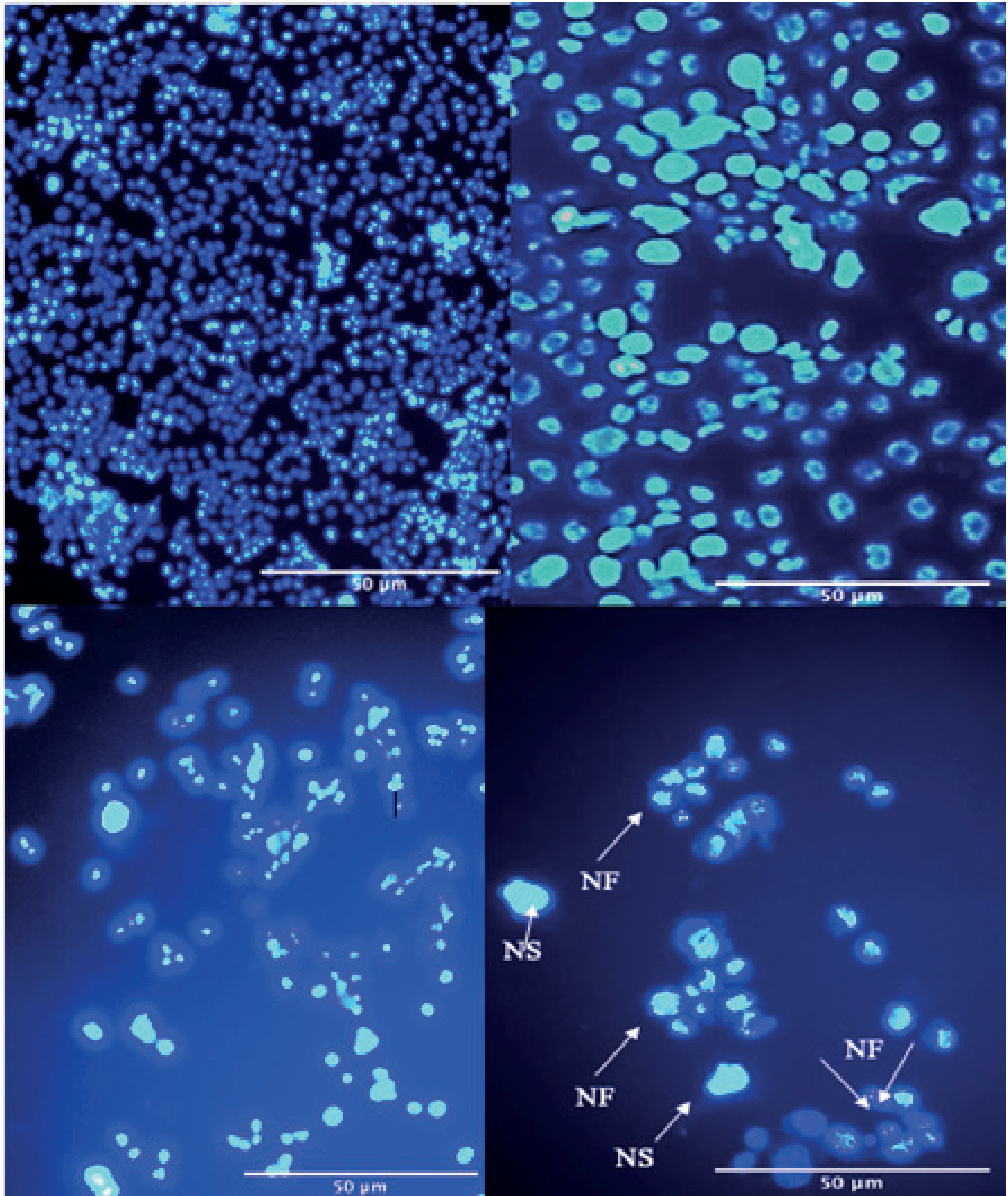


**Figure 3:** Cell morphology of DU-145 cells, control cells (A,B) were seen with uniformly light blue nuclei under fluorescence microscope; while Myo-inositol treated DU145 cells (C&D) exhibited nuclear shrinkage (NS) and nuclear fragmentation (NF). Pictures are in various magnifications (A) 40X, (B), 100X (C) 200X and (D) 400 X.



upon treatment until only 9.71% of viable cells were left on day 8. Treatment with myo-inositol resulted moderate cell viability 77.05% (\*\* $p < 0.05$ ) in 24 hours, whereas; it suppressed cell viability 90.29% (\*\* $p < 0.001$ ) of the cells relative to the untreated cells.

The image of untreated DU-145 cells showed the characteristics of well-differentiation, normal nucleus cytoplasm ratio, and regular membrane profile characteristics in Figure 2(a). Moreover, light microscopy analysis in Figure 2 (b) shows that the treated samples have definite apoptosis characteristics, such as vacuolation (a), cell elongation (b), cell shrinkage (c), apoptotic bodies (d) and membrane blebbing, after 72 hours of treatment following the  $IC_{50}$  dose of Myo-Inositol. In addition, direct observations with an inverted light microscope showed that the cells treated with Myo-inositol decreased in number and had major transformations that could be separated from the untreated cell control group.

#### Hoechst 33342 staining analysis of apoptosis

Figure 3, shows Hoechst 33342 staining carried out to investigate the apoptosis induction of Myo-inositol on DU-145 cells treated with  $IC_{50}$  doses for 72 hours. After treatment with Hoechst 33342, control cells were seen with uniformly light blue nuclei under fluorescence microscope; while Myo-inositol treated DU-145 cells exhibited nuclear shrinkage (**NS**) and nuclear fragmentation (**NF**).

#### DNA fragmentation analysis

As shown in the figure 4, DNA fragmentation assay was used to determine the DU-145 cells underwent apoptosis after being treated with Myo-inositol. Morphological features such as plasma membrane condensation reduction of nuclei and inter-nucleosomal division of DNA (the genome is cleaved at inter nucleosomal locations, generating a 'ladder' of DNA fragments when analysed by agarose gel electrophoresis) are included in the characteristics of apoptosis. Standard agarose gel electrophoresis reveals apoptosis as a ladder pattern of 100-20 bp due to DNA breakage by nuclear activation endonuclease. After 72 hours of treatment with an  $IC_{50}$  dose of Myo-inositol, the isolation of DNA from DU-145 cells was significantly higher that of DNA isolated from untreated cells (individual DNA fragments can be measured by graphing their molecular weight logs against their travel distance).

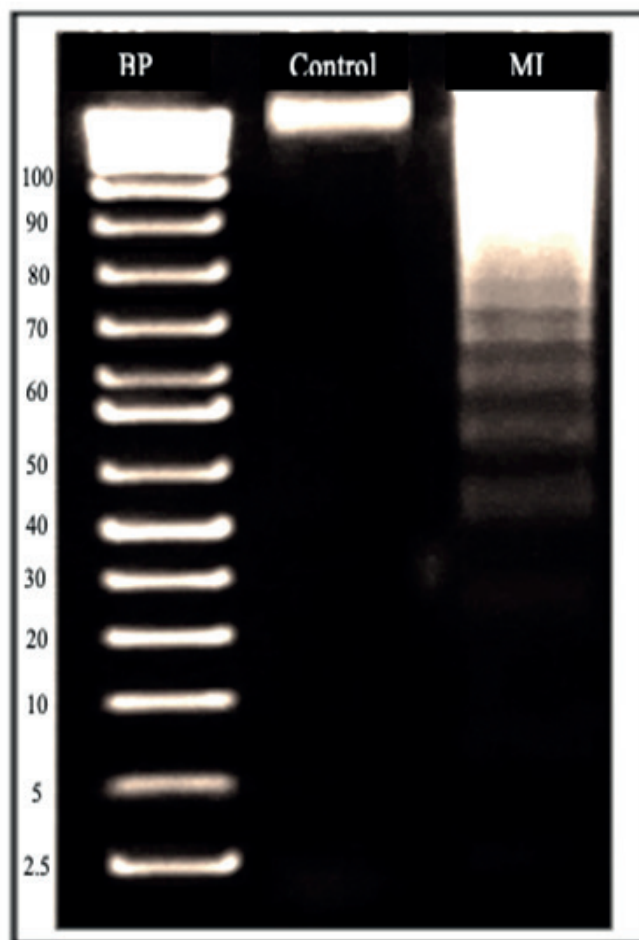


**Figure 4:** Agarose gel electrophoresis for DNA fragmentation assay (apoptotic ladder) showing Lane 1 (DNA ladder 100bp), Lane 2 (control), Lane 3 (DNA isolated from Myo-inositol treated cells), indicated there were fragmentation (apoptotic ladder) after treatment with Myo-inositol for 72 hours.

#### Effect of Myo-inositol on apoptosis induction of DU-145 cell line

An apoptosis study with flow cytometry 72 hours after treatment further confirmed the inhibitory effect of Myo-inositol. Myo-inositol treated cells were flow cytometrically examined after being stained with annexin-V tagged fluorescein isothiocyanate (FITC) and propidium iodide (PI). The percentage of DU-145 live cells (\*\* $p < 0.01$ ) from 86.33% (untreated) to 59.00% was significantly reduced by Myo-inositol treated cells. This suggests that treatment with Myo-inositol impaired DU-145 cell proliferation and consequently reduced the percentage of living cells. Myo-inositol treatment induced 17.83% (\*\* $p < 0.01$ )

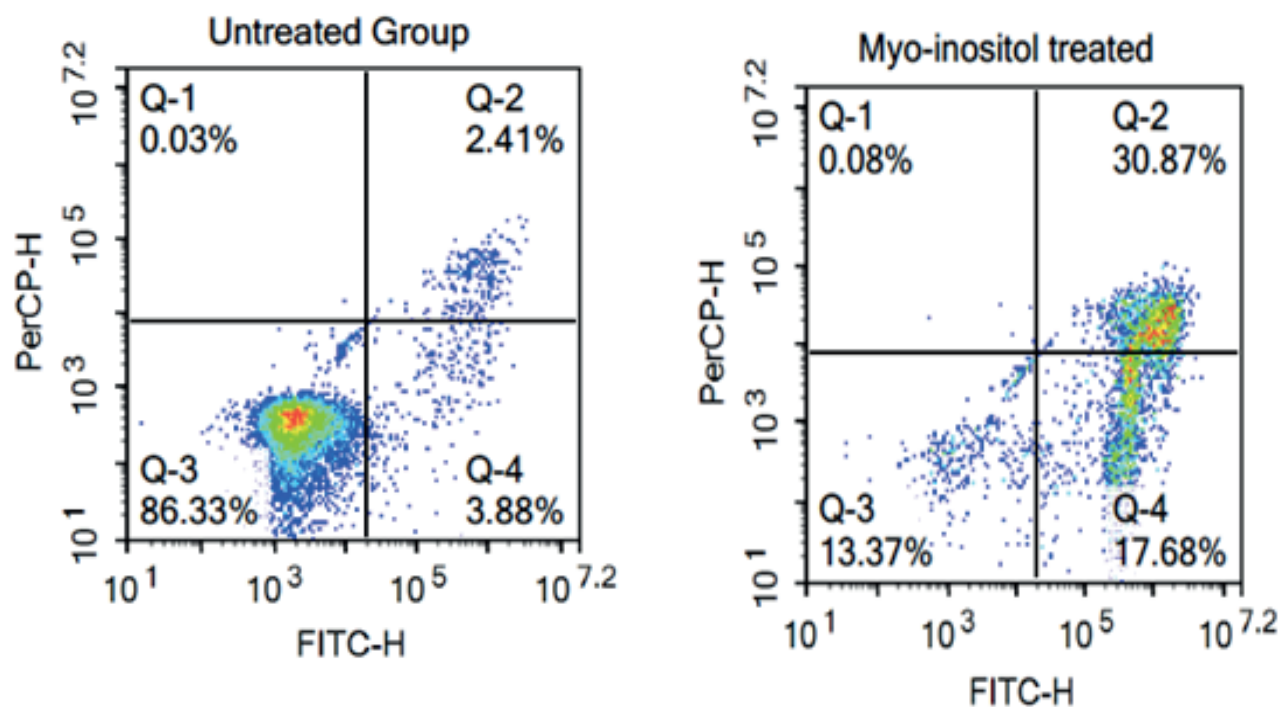


**Figure 5:** Showing cell apoptosis induction in response to myo-inositol treatment.

of early apoptosis, which was 9.23% higher than the untreated group of cells, which could be the primary cause of such effect. In addition, Myo-inositol treatment induced 30.06% late apoptosis, which was nearly 24% higher than untreated cells. The percentage of apoptotic cells in the population of untreated and treated DU-145 cells obtained after data analysis from three separate tests is shown in figure 5.

#### Effect of Myo-inositol on cell-cycle progression of DU-145 cell line

Observations of the cell cycle arrest induced by Myo-Inositol in the DU-145-cell line were reported in this experiment. After treatment of Myo-inositol cells at the  $IC_{50}$  dose and staining with propidium iodide (PI) after 72 hours of incubation, cell cycle analysis was carried out by flow cytometry. PI is a fluorescent molecule that can migrate across cell membranes, and using flowing cytometry, fluorescent-activated cell selection (FACS) can detect and quantify intercepts in cellular DNA. The amount of PI in cells thus reflects the amount of DNA, and it is able to quantify the location of the cell cycle of the cells. MODFIT software was used to analyze the raw data for the flow cytometer.

There were three control points in the cell cycle, phase  $G_0 / G_1$ , phase S and phase  $G_2/M$ . The distribution and ratio of cell cycles in DU-145 cells treated with Myo-inositol are shown in figure 6, most of the cells were in the  $G_1$  phase without the treatment of Myo-inositol (untreated cells)  $52.00 \pm 1.76\%$ , and  $33.92 \pm 0.12\%$ , at the S and  $G_2/M$  stages respectively. After exposure to the  $IC_{50}$  Myo-inositol dose, the percentage increased significantly in the  $G_0/G_1$ , and S phases, which was 70.07%, and 23.40% cell cycle, respectively, were the outcomes of DU-145 cells with treatment. Myo-inositol treatment didn't produce any significant changes with the  $G_2/ M$  stages of cell-cycle arrest.

#### DISCUSSION

Due to their bioactive components and physiological benefits, herbs and plants are often consumed. They can be used in a variety of forms, including teas, syrups, ointments, and pills. Due to the negative side effects of chemotherapy, alternative cancer treatments derived from natural substances have been extensively explored and found to be effective. Myo-inositol suppresses the growth of human leukaemia, colon, breast, prostate, and hepatoma cell lines. Growth of mouse

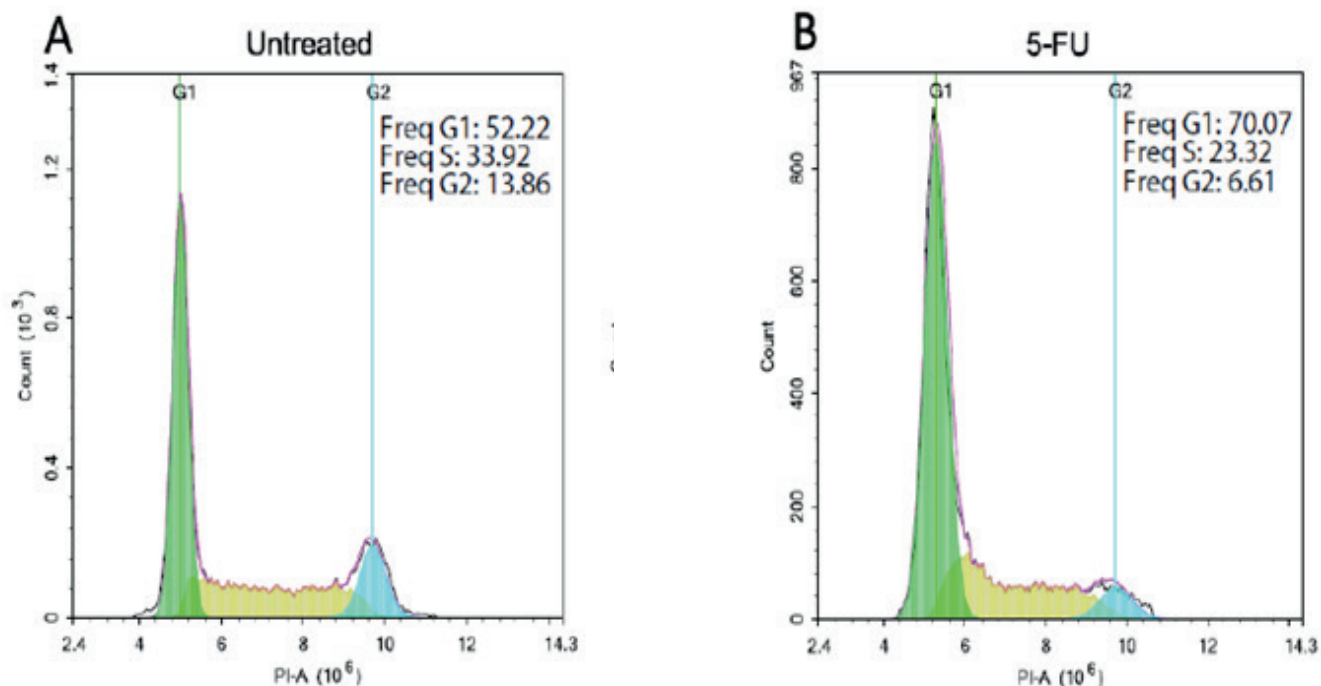


**Figure 6:** Showing cell cycle analysis in response to myo-inositol treatment.

fibrosarcoma, colon, mammary, lung tumor and human rhabdomyosarcoma are the examples of mesenchymal tumours inhibited by myo-inositol in vivo study.

Myo-inositol treatment via trypan blue exclusion assay (TBEA) has been shown to substantially suppress the proliferation of *in vitro* androgen-specific prostate cancer cell line (DU-145). For 72 hours, different doses of Myo-inositol were tested for their effects on DU-145 cells. A certain dose of DU-145 cell line induced 50% cell death from Myo-Inositol. The best  $IC_{50}$  value obtained was 0.06 mg/ml, resulting in 50% death of prostate cancer cells from DU-145. The findings indicate a statistically significant (\*\* $p < 0.05$ ) inhibitory effect of the compound on DU-145. This concentration is lower than the concentrations of myo-inositol identified in earlier research, which effectively treated breast cancer models in mice without causing any side effects and have a robust anti-cancer impact at 750  $\mu\text{g}/\text{mL}$  and 1500  $\mu\text{g}/\text{mL}$ .

The cytotoxic effect of Myo-inositol has been investigated in mouse skin fibroblast cell lines (L929) using TBEA in the current study. In a prior work by Khairunnisa *et al.*, 2014, showing that L929 fibroblast cells could provide appropriate screening models for

*in vitro* cytotoxicity evaluation and for the long term *in vitro* cytotoxicity test. Less than 11% of mouse skin fibroblast cell lines (L929) are inhibited after treatment with Myo-inositol at a dose of 0.06 mg/ml  $IC_{50}$  (Figure 4.6). According to ISO standard 10993-5:2009, a compound was graded as non-cytotoxic when cell viability is greater than 80%; mildly cytotoxic when cell viability is between 80% to 50%; moderately cytotoxic when cell viability is between 50% to 30%; and severely cytotoxic when cell viability is less than 30%. The treatment product compound should not inhibit cell proliferation by more than 30%, as this indicates a cytotoxic effect<sup>24</sup>.

In the present study, the results showed that Myo-inositol caused morphological changes of DU-145 cells related to the apoptosis such as elongation, shrinkage and the appearance of apoptotic bodies (Figure 4.3 b). A study on the effect of *Allium atrovioleceum* bulb extract on HeLa and HepG2 cell lines by Khazaei *et al.*, 2017, have shown that *Allium atrovioleceum* can induce apoptosis by a different mechanism at the molecular level, however, it showed a very alike surface morphological characters of apoptosis such as cell rounding up, blebbing and fragmentation. This result was consistent with the inhibition of cell count



associated with cell death via apoptosis under the treatment of Myo-inositol. Hoechst 33342 is a blue, permeable nucleic acid dye for fluorescent cells used to detect chromatin condensation and apoptotic cell fragmentation<sup>26</sup>. Apoptotic cell death is a characteristic of many therapies for diseases, including cancer, which results in the extracellular space release of DNA. In two different method, Hoechst 33342 dye binds to DNA stands: the high affinity (Kd1-10nM) binding results from the unique B-DNA minor groove interaction and the low affinity (Kd ~1000 nM) represents the non-specific DNA sugar-phosphate backbone interaction. The AAA/TTT sequence is the optimum binding site, and interaction with the dye does not affect the B-DNA structure<sup>27</sup>.

The presence of chromatin in a group of bright spherical blue beads indicates the early apoptosis process. Nuclear chromatin condensation accompanied by chromatin breakup leading to nuclear fragmentation is characterized by apoptosis. Nuclear shrinkage and chromatin condensation, which are characteristics of apoptosis, were found in the study significantly (\*\* $p < 0.01$ ) (Figure 4.4). The presence of chromatin in a group of bright spherical blue beads indicates the early apoptosis process. Other analyses, such as DNA fragmentation analysis, have confirmed the induction of apoptosis. DNA fragmentation is a critical feature of apoptosis that distinguishes apoptotic from necrotic cells. Nucleases, such as Caspases-activated DNase (CAD), are involved in DNA cleavage, resulting in a distinct ladder pattern on an agarose gel<sup>28,29</sup>. A biochemical hallmark of apoptotic cell death is DNA fragmentation. The DNA laddering method is used to visualize the apoptosis products of endonuclease cleavage<sup>30</sup>. This assay involves extraction of DNA from a lysed cell homogenate followed by agarose gel electrophoresis. This assay includes DNA extraction from a homogenate of a lysed cell accompanied by electrophoresis of agarose gel. This results in a characteristic 'DNA ladder' of approximately 180 base pairs divided in size by each band in the ladder. Myo-inositol treatment has significantly (\*\* $p < 0.01$ ) resulted in chromosomal DNA fragmentation into smaller fragments (Figure 4.7), which is the hallmark of apoptosis<sup>31</sup>.

According to Collins *et al.* (2019), when a mitochondrial membrane potential is lost, cytochrome c is released and caspases are activated. Translocation

**Table 1:** Myo-inositol treated DU-145 cell number and viability

Concentration (mg/ ml)	Cell number average (1 x 10 <sup>5</sup> cells)	Cell Viability (%)
0	13.20 ± 5.00	100.00 ± 0.00
0.02	10.16 ± 4.04	77.05±2.1
0.04	7.56 ± 5.51	57.32±1.8
<b>0.06</b>	<b>6.63 ± 5.03</b>	<b>50.26±1.2</b>
0.08	5.83 ± 3.06	44.22±0.7
0.10	4.30 ± 7.94	32.46±1.1

of phosphatidylserine (PS) from the inner to outer leaflet of the cell exposes it to the extracellular environment<sup>32</sup>. Early apoptotic cells represented by the Q3 quadrant's phosphatidylserine (PS) that is exposed are bound by annexin V. Furthermore, the integrity and selective transport of materials are compromised by the permeability of cellular membranes. A DNA-binding dye called PI (Propidium Iodide) is used to identify late-apoptotic cells in the Q4 quadrant. In order to determine whether the cells were undergoing apoptosis or not, the percentage of apoptotic cells in DU-145 cell line treated flow cytometry were examined in the current study. The findings demonstrated that early and late apoptosis had substantial percentages of total apoptosis in both early and late phases ( $p > 0.01$ ) (Figure 6).

In this analysis, with the treatment of Myo-inositol compounds in DU-145 cells, cell cycle distribution was investigated. Here in flow cytometry analysis results showed that the Myo-inositol compound at a concentration of 0.06 mg/ml could inhibit statistically significant (\*\* $p < 0.01$ ) cell evolution throughout cell cycle arrest specifically at the G<sub>0</sub>/G<sub>1</sub> and S phase (Table 4.3). According to Doan *et al.*, 2019, the end result of all growth-promoting stimulus is the entry of quiescent cells into the cell cycle, as a result the first gap step (G<sub>1</sub>) and initiation of synthesis (S phase) are regulated in the mammalian division cycle, by several groups of cyclin-dependent kinases (CDK) triggered by cyclins and their activities otherwise restricted by cycle-dependent inhibitors (CDKIs).

In conclusion, the findings of this study demonstrate

the potent anti-cancer effects of Myo-inositol on DU-145 cells. The  $IC_{50}$  dose was determined to be 0.06 mg/ml, and Myo-inositol treated samples exhibited distinct apoptosis characteristics. Nuclear shrinkage and fragmentation were observed in the Myo-inositol treated cells stained with Hoechst 33342, indicating apoptotic cell death. Moreover, DNA isolation from Myo-inositol treated cells showed a significant increase in comparison to untreated cells, further supporting the induction of apoptosis.

Flow cytometric analysis using annexin-V-FITC and PI staining revealed a considerable increase in both early (17.83%; \*\*\* $p < 0.01$ ) and late (30.06%) apoptosis in Myo-inositol treated cells compared to untreated cells, with a 9.23% and 24% higher rate, respectively. These results suggest that Myo-inositol is primarily responsible for inducing apoptosis in DU-145 cells. Additionally, Myo-inositol treatment led to the arrest

of cell cycle progression at the G1-S phase, further inhibiting cell proliferation.

Taken together, these findings provide substantial evidence for the potential therapeutic use of Myo-inositol in treating prostate cancer. Further research is warranted to elucidate the molecular mechanisms underlying the pro-apoptotic effects of Myo-inositol and to explore its potential as a novel therapeutic agent in the management of prostate cancer.

**Source of Fund:** Not applicable.

**Conflict of interest:** In this original article there is no potential conflict of interest.

**Ethical clearance:** Not applicable.

**Authors contribution:** All the authors contributed equally to this review paper.

## REFERENCES

- Gulland A. Global cancer prevalence is growing at “alarming pace,” says WHO. *BMJ : British Medical Journal*. 2014;**348**:g1338. doi:10.1136/bmj.g1338
- Yusof N, Yasin NM, Yousuf R, Wahab AA, Aziz SA. Comparison of neutrophil respiratory oxidative burst activity between flow cytometry using dihydrorhodamine (DHR) 123 and conventional nitroblue tetrazolium test (NBT). *Bangladesh Journal of Medical Science*. 2022;**21**(3):626-633. doi:10.3329/bjms.v21i3.59577
- Xi Y, Xu P. Global colorectal cancer burden in 2020 and projections to 2040. *Translational Oncology*. 2021/10/01/2021;14(10):101174. doi:<https://doi.org/10.1016/j.tranon.2021.101174>
- Momin MAB, Aluri A, Reddy GVK, Singh RD. Primary Plasma Cell Leukaemia with Lambda Light Chain secretion and Chromosomal abnormalities presenting as hyperleukocytosis - A case report. *Bangladesh Journal of Medical Science*. 2023;**22**(4):932-936. doi:10.3329/bjms.v22i4.67118
- Stepas J, Sokhor N, Shkrobot L, Holovatiuk L, Marushchak M, Krynytska I. Features of leukocytes' apoptosis and emoxypine succinate efficacy in case of combined trauma of the chest and both thighs in rats. *Bangladesh Journal of Medical Science*. 2019;**18**(2):244-251. doi:10.3329/bjms.v18i2.40693
- Ha Chung B, Horie S, Chiong E. The incidence, mortality, and risk factors of prostate cancer in Asian men. *Prostate International*. 2019/03/01/ 2019;**7**(1):1-8. doi:<https://doi.org/10.1016/j.pnil.2018.11.001>
- Nurseta T, Harumsari S, Prasetya NA, Indrawan IWA. All-Trans Retinoic Acid Reduces Matrix Metalloproteinase-2 and Increases E-Cadherin Levels in BeWo Choriocarcinoma Cells. *Bangladesh Journal of Medical Science*. 2023;**22**(2):336-340. doi:10.3329/bjms.v22i2.64992
- Fuadi AF, Riwanto I, Putra A, Prabowo E, Istiadi H. Mesenchymal Stem Cells Combined with Bovine Colostrum Decrease the PDGF and Fibrosis Level after Hepatectomy in Liver Fibrosis Rats Model. *Bangladesh Journal of Medical Science*. 2022;**21**(2):262-270. doi:10.3329/bjms.v21i2.58057
- Key TJ, Bradbury KE, Perez-Cornago A, Sinha R, Tsilidis KK, Tsugane S. Diet, nutrition, and cancer risk: what do we know and what is the way forward? *Bmj*. Mar 5 2020;**368**:m511. doi:10.1136/bmj.m511
- Arjana AZ, Devita N, Marfianti E, Rosita L. CD40L-CD40 interaction avidity as coronary artery disease predictive factor. *Bangladesh Journal of Medical Science*. 2021;**20**(4):796-800. doi:10.3329/bjms.v20i4.54137
- Bizzarri M, Dinicola S, Bevilacqua A, Cucina A. Broad Spectrum Anticancer Activity of Myo-Inositol and Inositol Hexakisphosphate. *Int J Endocrinol*. 2016;2016:5616807. doi:10.1155/2016/5616807
- Shafie NH, Mohd Esa N, Ithnin H, Md Akim A, Saad N, Pandurangan AK. Preventive Inositol Hexaphosphate Extracted from Rice Bran Inhibits Colorectal Cancer through

- Involvement of Wnt/ $\beta$ -Catenin and COX-2 Pathways. *BioMed Research International*. 2013/10/24 2013;2013:681027. doi:10.1155/2013/681027
13. Teli M, Niyaz M, Rashid G, Parveiz I, Wani RA, Mudassar S. Hypomethylation of Sonic hedgehog in colorectal cancer. *Bangladesh Journal of Medical Science*. 2024;**23**(1):200-206. doi:10.3329/bjms.v23i1.70719
  14. Vucenik I, Druzijanic A, Druzijanic N. Inositol Hexaphosphate (IP6) and Colon Cancer: From Concepts and First Experiments to Clinical Application. *Molecules*. Dec 15 2020;**25**(24) doi:10.3390/molecules25245931
  15. Ahmad R, Haque M. Obesity inflicted reproductive complications and infertility in men. *Bangladesh Journal of Medical Science*. 2023;**22**(1):7-14. doi:10.3329/bjms.v22i1.63075
  16. Shen D, Ju L, Zhou F, *et al*. The inhibitory effect of melatonin on human prostate cancer. *Cell Communication and Signaling*. 2021/03/15 2021;**19**(1):34. doi:10.1186/s12964-021-00723-0
  17. Bhandary S, Shetty MS, Sharma D, Tanna DA, Jain M. The Medicinal Chemistry of Curcuma Longa : A Narrative Review. *Bangladesh Journal of Medical Science*. 2023:67-71. doi:10.3329/bjms.v22i20.66312
  18. Adan A, Kiraz Y, Baran Y. Cell Proliferation and Cytotoxicity Assays. *Curr Pharm Biotechnol*. 2016;**17**(14):1213-1221. doi: 10.2174/1389201017666160808160513
  19. Chodidjah, Dharmana E, Susanto H, Ekawuyung P. The effect of the ethanol extract of Typhonium flagelliforme on apoptosis adenocarcinoma mamma cells in C3H mice. *Bangladesh Journal of Medical Science*. 2023;**22**(2):329-335. doi:10.3329/bjms.v22i2.64991
  20. Chen E, Cario CL, Leong L, *et al*. Cell-free DNA concentration and fragment size as a biomarker for prostate cancer. *Sci Rep*. Mar 3 2021;**11**(1):5040. doi:10.1038/s41598-021-84507-z
  21. Allen JE, Hart LS, Dicker DT, Wang W, El-Deiry WS. Visualization and enrichment of live putative cancer stem cell populations following p53 inactivation or Bax deletion using non-toxic fluorescent dyes. *Cancer Biol Ther*. Nov 2009;**8**(22):2194-205. doi:10.4161/cbt.8.22.10450
  22. Murad H, Hawat M, Ekhtiar A, *et al*. Induction of G1-phase cell cycle arrest and apoptosis pathway in MDA-MB-231 human breast cancer cells by sulfated polysaccharide extracted from *Laurencia papillosa*. *Cancer Cell International*. 2016/05/26 2016;**16**(1):39. doi:10.1186/s12935-016-0315-4
  23. Pumiputavon K, Chaowasku T, Saenjum C, *et al*. Cell cycle arrest and apoptosis induction by methanolic leaves extracts of four Annonaceae plants. *BMC Complementary and Alternative Medicine*. 2017/06/05 2017;**17**(1):294. doi:10.1186/s12906-017-1811-3
  24. López-García J, Lehocký M, Humpolíček P, Sába P. HaCaT Keratinocytes Response on Antimicrobial Atelocollagen Substrates: Extent of Cytotoxicity, Cell Viability and Proliferation. *J Funct Biomater*. May 8 2014;**5**(2):43-57. doi:10.3390/jfb5020043
  25. Khazaei S, Esa NM, Ramachandran V, *et al*. In vitro Antiproliferative and Apoptosis Inducing Effect of Allium atroviolaceum Bulb Extract on Breast, Cervical, and Liver Cancer Cells. Original Research. *Frontiers in Pharmacology*. 2017-January-31 2017;**8**(5)doi:10.3389/fphar.2017.00005
  26. Gruenwedel DW. NUCLEIC ACIDS | Properties and Determination. In: Caballero B, ed. *Encyclopedia of Food Sciences and Nutrition (Second Edition)*. Academic Press; 2003:4147-4152.
  27. Doan P, Musa A, Candeias NR, Emmert-Streib F, Yli-Harja O, Kandhavelu M. Alkylaminophenol Induces G1/S Phase Cell Cycle Arrest in Glioblastoma Cells Through p53 and Cyclin-Dependent Kinase Signaling Pathway. Original Research. *Frontiers in Pharmacology*. 2019-April-02 2019;10doi:10.3389/fphar.2019.00330
  28. Saraste A, Pulkki K. Morphologic and biochemical hallmarks of apoptosis. *Cardiovascular Research*. 2000;**45**(3):528-537. doi:10.1016/S0008-6363(99)00384-3
  29. Kamalidehghan B, Ahmadipour F, Noordin MI. DNA fragmentation is not associated with apoptosis in zerumbone-induced HepG2 cells. *Iran Biomed J*. 2012;**16**(4):226.
  30. Jamali T, Kavooosi G, Safavi M, Ardestani SK. In-vitro evaluation of apoptotic effect of OEO and thymol in 2D and 3D cell cultures and the study of their interaction mode with DNA. *Scientific Reports*. 2018/10/25 2018;**8**(1):15787. doi:10.1038/s41598-018-34055-w
  31. Khairunnisa K, Karthik D. Evaluation of in-vitro apoptosis induction, cytotoxic activity of Hymenodictyon excelsum (Roxb) Wall in Dalton's lymphoma ascites (DLA) and Lung fibroblast - Mouse L929 cell lines. *Journal of Applied Pharmaceutical Science*. 09/04 2014;**4**:011-017. doi:10.7324/JAPS.2014.40803
  32. Bilen MA, Martini DJ, Liu Y, *et al*. The prognostic and predictive impact of inflammatory biomarkers in patients who have advanced-stage cancer treated with immunotherapy. *Cancer*. Jan 1 2019;**125**(1):127-134. doi:10.1002/cncr.31778
  33. Doan P, Musa A, Candeias NR, Emmert-Streib F, Yli-Harja O, Kandhavelu M. Alkylaminophenol Induces G1/S Phase Cell Cycle Arrest in Glioblastoma Cells Through p53 and Cyclin-Dependent Kinase Signaling Pathway. Original Research. *Frontiers in Pharmacology*. 2019-April-02 2019;**10**(330) doi:10.3389/fphar.2019.00330